Langevin equation elucidates the mechanism of the Rayleigh-Bénard instability by coupling molecular motions and macroscopic fluctuations

Jun Zhang*
School of Aeronautic Science and Engineering, Beihang University, Beijing 100191, China

Thomas Önskog
Department of Mathematics, KTH Royal Institute of Technology, Stockholm SE-100 44, Sweden
(Received 2 May 2017; revised manuscript received 27 July 2017; published 9 October 2017)

It is well known that Brownian motion can be described using Langevin equation. In this paper we extend the application of the Langevin equation to the Rayleigh-Bénard (RB) flow, assuming that each molecule in the system is a Brownian particle colliding with its surrounding molecules. The phenomenon of thermal instability, changing from a conductive to a convective state, is well reproduced by Langevin dynamics simulations. The roles of the drag force and the random force terms in the Langevin equation in triggering thermal instability are elucidated via numerical tests. Furthermore, we demonstrate that the strength of the fluctuation correlations increases as the Rayleigh number approaches the critical value, and the characteristics of the fluctuation correlations below the onset of instability foreshadow the form of the convective patterns emerging above the critical point. The Langevin equation, together with the form of the fluctuation correlations, sheds new light on the mechanism of the RB instability.

DOI: 10.1103/PhysRevE.96.043104

I. INTRODUCTION

The Rayleigh-Bénard (RB) system—a fluid confined between two horizontal parallel plates that are heated from below or cooled from above—is a paradigm in the studies of hydrodynamic instability, pattern formation, and nonlinear dynamics and chaos. Since the seminal experimental work of Bénard in 1900 and the linear stability analysis of Rayleigh in 1916 (for a review of the early studies, see Chandrasekhar's monograph [1]), there have been numerous studies on this subject including experiments, theoretical analyses, and numerical simulations [2,3].

Now it is well known that the occurrence of the RB instability under the conditions of Boussinesq approximation can be predicted by one dimensionless control parameter, namely, the Rayleigh number (Ra),

$$\mathrm{Ra} = \frac{\alpha g d^3 \Delta T}{\nu \kappa}, \tag{1}$$

where α, ν, and κ are the isobaric thermal expansion coefficient, kinematic viscosity, and thermal diffusivity, respectively, g is the acceleration of gravity, d is the height of the fluid layer, and $\Delta T = T_h - T_c$ is the temperature difference between the lower and upper plates. As long as Ra is not too large, the fluids remain quiescent and heat is transported only by conduction. If Ra exceeds the critical value $\mathrm{Ra_c} \approx 1708$, however, instability sets in and a well-ordered convection structure appears.

A fundamental question to be asked about the RB system is this: How does the well-ordered spatial pattern arise out of the disordered state of molecules or atoms? A lot of efforts have been made over the past half century aiming to answer this question. Dissipative structure theory proposed by Prigogine [4] and synergetics founded by Haken [5] might be two of the most successful theories for explaining the formation of the self-organizing structure. Prigogine considered RB instabilities from the standpoint of irreversible thermodynamics. He stated that the distance from equilibrium and the nonlinearity were the sources capable of driving the system to an ordered configuration. Haken's theory particularly investigates what happens at the instability point and determines the new structure beyond it. According to synergetics, when the system is close to the instability point, a new set of collective variables can be identified as the "order parameters," which determine the system's behavior. Note that both the dissipative structure theory and synergetics are still at the macroscopic scale, so they cannot explain from a microscopic point of view how the molecules or atoms in a disordered state change to an ordered state above the critical point.

Rapid development in high performance computing over the past three decades has made it possible to study hydrodynamic instability [6,7] and even turbulence [8] at the microscopic level using molecular simulation methods, where the dynamics of molecules or atoms are explicitly calculated and the macroscopic fluid properties are obtained as averages over the trajectories of the particles. Two of the most popular molecular simulation methods, the direct simulation Monte Carlo (DSMC) method and the molecular dynamics (MD) method, have been employed to study the RB convection in gases [9,10] and liquids [11,12], respectively. Basically, very good agreement between molecular simulations and macroscopic continuum simulations has been demonstrated for the RB convection. The advantage of molecular simulations is that molecular thermal motions are inherently involved, so it is convenient to investigate the role of the thermal fluctuations in the RB instability [10,13]. In contrast to the short-range characteristic in equilibrium, the thermal fluctuations in the RB system are long-range correlated [14], and this has been proved to be important for the occurrence of instability, especially near the critical point [15].

However, due to the enormous requirement of the computational resources for the molecular simulations of the

*jun.zhang@buaa.edu.cn

RB flow, the spatial scale achieved in the current molecule simulations is still several orders smaller than those in experiments. More importantly, individual molecular information is not directly connected to macroscopic phenomena such as thermal instability, as there is a clear scale gap between the individual molecular motions and macroscopic motions. Molecular information needs to be averaged to get macroscopic quantities, which are then used to explain macroscopic phenomena.

In this paper, a coarse-grained particle simulation method based on the Langevin equation is employed to investigate the RB flows, by assuming that each molecule in the system is a Brownian particle colliding with its surrounding molecules on the time scale larger than molecular mean collision time. Instead of considering the details of intermolecular collisions or forces in conventional molecular simulation methods, the Langevin equation uses two coarse-grained force terms, i.e., a drag force and a random force term, to describe a continuous stochastic process in any direction for one molecule as follows:

$$\frac{du_i}{dt} = -\frac{1}{\tau}(u_i - U_i) + \left(\frac{2R_sT}{\tau}\right)^{1/2}\frac{dW_i(t)}{dt} + g\delta_{iy}, \quad (2)$$

where u and U are the molecular velocity and the local macroscopic velocity, respectively, the subscript i denotes the direction of a vector, τ is the characteristic relaxation time, R_s is the specific gas constant, T is the local temperature, $W(t)$ refers to a Wiener process, and δ_{iy} denotes that the gravity acceleration g only exerts on the y direction. Note that the increment $dW(t)$ of the Wiener process is normally distributed with expectation zero and variance dt. Equivalently, $dW(t)$ is equal to the product of $\sqrt{dt}$ and a standard normally distributed random variable with expectation zero and unit variance. According to the theory of stochastic processes, the Langevin equation is equivalent to the Fokker-Planck equation for the probability density function. In this context, the Langevin dynamics described by Eq. (2) can be considered as a particle Fokker-Planck model. Originally, Jenny *et al.* [16] proposed a stochastic particle Fokker-Planck algorithm based on Eq. (2) for simulations of rarefied gas flows. Afterwards, Gorji and Jenny [17] developed a more efficient algorithm. Two critical issues related to Langevin dynamics simulations, i.e., how to get correct transport properties and how to deal with boundary conditions, have been successfully solved by Gorji *et al.* [18] and Önskog and Zhang [19], respectively. The latest progress demonstrated the ability of the Langevin dynamics simulations to study large-scale flows [20].

Here we apply the Langevin equation to study RB flows. Our aim is to elucidate the mechanism of the occurrence of macroscopic structure arising out of a disordered state, from the viewpoint of molecular movements. It can be seen from Eq. (2) that the drag force term in the Langevin equation makes the microscopic molecular velocity tend to the local macroscopic velocity, while the random force term behaves as a source adding fluctuations to the molecular velocity. Therefore, it offers a way to study the RB instability by connecting the microscopic and macroscopic information.

II. SIMULATION MODEL AND COMPUTATIONAL CONSIDERATIONS

We employ the Langevin model as Eq. (2) to simulate two-dimensional RB argon gas flows with the aspect ratio $\Gamma = L/d = 2.0$; that is, the ratio of the length along the horizontal direction to the height along the normal direction is 2.0. Previous studies using the DSMC method [9,21] and linear stability analysis [22] have demonstrated that, for the compressible RB gas flows, the instability is not governed by the single Rayleigh parameter, but governed by the temperature ratio $r = T_c/T_h$, the Knudsen number Kn, and the Froude number Fr. Note that in the Langevin model, there is only one parameter, i.e., the relaxation time τ defined explicitly. In order to derive the expression of the Rayleigh number in terms of the temperature ratio, the Knudsen number, and the Froude number, we employ the hard-sphere model [23], which is popularly used in the kinetic theory and particle simulation methods, to give an explicit relationship between transport coefficients and molecular mean free path. On this point, our simulation model can be regarded as a combined Langevin hard-sphere model.

Based on the state equation of a perfect gas, the isobaric thermal expansion coefficient is dependent on temperature as

$$\alpha = \frac{1}{V}\left(\frac{\partial V}{\partial T}\right)_p = \frac{1}{T}, \quad (3)$$

where V denotes the volume of gas, and p is pressure.

According to the kinetic theory, for a hard-sphere gas, the viscosity coefficient is related to the molecular mean free path as follows [23]:

$$\nu = \frac{5\sqrt{\pi}}{16}\lambda\bar{c}, \quad (4)$$

where λ is the molecular mean free path, and $\bar{c} = \sqrt{2R_sT}$ is the most probable molecular thermal speed. Previous studies have demonstrated that the linear Langevin model predicts the Prandtl number (Pr) of gas as 3/2 [16,24], and hence the thermal diffusivity coefficient for our model is

$$\kappa = \frac{5\sqrt{\pi}}{24}\lambda\bar{c}. \quad (5)$$

Considering the temperature difference between the two plates, we use the average temperature $T = (T_c + T_h)/2$ in Eqs. (3)–(5). Substituting Eqs. (3)–(5) into Eq. (1) yields

$$\mathrm{Ra} = \frac{1536}{25\pi} \times \frac{1-r}{(1+r)^2\mathrm{Kn}^2\mathrm{Fr}}, \quad (6)$$

where the temperature ratio is $r = T_c/T_h$, the Knudsen number is $\mathrm{Kn} = \lambda/d$, and the Froude number is $\mathrm{Fr} = \bar{c}_h^2/gd$. Note that the form of Eq. (6) is the same as that derived in previous DSMC investigations [9,25], and the only difference lies in the value of the prefactor due to the fact that the linear Langevin model in Eq. (2) predicts Pr to be 3/2 instead of 2/3 [24]. Of course we can use a nonlinear Langevin model to get the correct Pr for monatomic gas molecules [18]. However, in this paper our focus is to study the mechanism of the RB instability, so we keep to the linear Langevin model for simplicity.

Our Langevin dynamics simulation is performed under the fixed condition of $r = 0.1$ and $\mathrm{Kn} = 0.01$, and the variation of

Ra is realized by adjusting Fr, more concretely, by changing the strength of gravity as in previous DSMC investigations [9,25]. The two-dimensional simulation box is 13.74 μm $\times$ 6.87 μm and is divided into 256 $\times$ 128 computational cells. At the initial time, the gas number density is 2.44×10^{25} m^{-3}, and the gas temperature is the same as the temperature of the lower plate (300 K). This means that in our simulation setup the RB flow is cooled from above. In each computational cell, 700 simulation molecules are assigned initially, with one simulated molecule representing 1.0×10^8 real molecules. The initial positions of the simulated molecules in one cell are uniformly and randomly distributed, while the initial velocities of the simulated molecules are sampled uniformly and randomly from a Maxwell distribution function at 300 K.

The calculation time step is set as 0.1τ. At every time step, the required instantaneous local macroscopic quantities including velocity and temperature in Eq. (2) are determined by sampling molecular information in the computational cells. To obtain the instantaneous local relaxation time, we first determine the local viscosity coefficient according to the calculated local temperature by using the characteristic of the hard-sphere model, i.e., $\nu/\nu_{\rm ref} = (T/T_{\rm ref})^{1/2}$ [23], with $\nu_{\rm ref} = 1.19\,{\rm m}^2\,{\rm s}^{-1}$ at $T_{\rm ref} = 273$ K for the argon gas model used here. We then determine the local relaxation time using the property of the Langevin model, i.e., $\tau = 2\nu/R_sT$ [16,24]. Having the local temperature, macroscopic velocity, and relaxation time determined, the Langevin equation as Eq. (2) can be solved by using the standard algorithm proposed by Jenny *et al.* [16]. For our two-dimensional (2D) simulations, the positions in the x and y directions and velocities in all three directions of the simulated molecules are then updated at every time step according to the solutions of the Langevin equation. Diffuse reflections are assumed at the upper and lower walls. It means that molecules colliding with a wall are reflected with the velocities sampled uniformly and randomly from a half-range Maxwellian distribution at the temperature of the wall. Periodic boundary conditions are adopted for both sides in the horizontal directions.

III. RESULTS AND DISCUSSIONS

We use the temporal evolution of the heat flux through the entire lower plate to monitor the instability process of the RB system, as shown in Fig. 1. The instant heat flux is an average value over a short time period $t_s = 100\tau$, by sampling the difference between the incident energy and the reflected energy of the molecules colliding with the lower plate. For the two cases with Ra = 1200 and Ra = 1600, after a short time period of oscillation (about $100t_s$), the heat flux reaches a constant value. This state corresponds to pure thermal conduction, where there are no macroscopic motions, and the temperature and density distributions along the horizontal direction are uniform, as shown in Figs. 2(a) and 2(b) for the case of Ra = 1600. Note that the results for steady state shown in Fig. 2 as well as Fig. 3 are obtained by taking an average over a time period of $100t_s$ or, equivalently, $10\,000\tau$. For the other three cases with larger Ra, however, the heat flux does not stay with the conductive value but increases to a new value after a transition period. Correspondingly, a steady convective pattern is formed and the temperature and density distributions

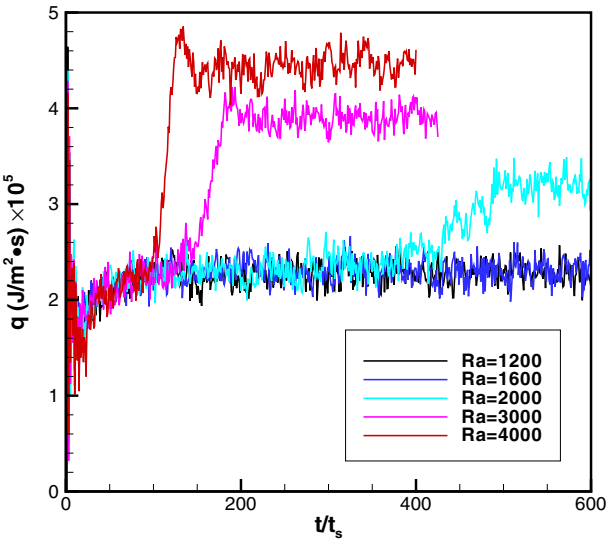

FIG. 1. The temporal evolution of the heat flux through the entire lower plate at various Ra.

are no longer uniform in the horizontal direction, as shown in Figs. 2(c) and 2(d) for the case of Ra = 4000.

Obviously, the heat flux in the convective state increases with Ra as shown in Fig. 1. We further compare our simulation results with theoretical and experimental results in terms of the Nusselt number (Nu), which is defined as the ratio of the heat flux to that in a pure conductive state. Figure 3 shows the relation between Nu $\times$ Ra and Ra. The curve is based on Schlüter *et al.*'s theoretical analysis [26] for the gas with Pr = 0.71 and $\mathrm{Ra_c} = 1708$. Below $\mathrm{Ra_c}$, the slope of the curve is 1.0, as Nu in the conduction state is always 1.0. Above $\mathrm{Ra_c}$, the slope changes to 2.41. The experimental data given by Koschmieder and Pallas [27] show that $\mathrm{Ra_c} \approx 1675$, and the data points are quite close to the theoretical curve. Overall, our simulation results are in agreement with the theory and experiment. The predicted $\mathrm{Ra_c}$ is about 1800, which is a little bit larger than the theoretical value (1708) and the experimental prediction. The reason for this is that the temperature and density variations in our simulations are relatively large, as shown in Fig. 2, and thus the effect of gas compressibility makes our simulations depart from the Boussinesq approximation, on which the theory and experiment were carried out. This non-Boussinesq effect has also been reported by using the DSMC method [9,21] and linear stability analysis of compressible macroscopic equations [22]. Our results are consistent with their conclusions under the condition of $r = 0.1$ and Kn = 0.01.

The aforementioned results demonstrate that Langevin dynamics simulations using Eq. (2) can predict the RB instability quite well, although the model looks very simple. In the Langevin equation, there are three forces exerted on each molecule, specifically, the drag force, the random force, and the gravity. The former two forces exist in both directions, while gravity is along the vertical direction. The roles of these three forces are different. Gravity accelerates all molecules downwards in the vertical direction, until they collide with the lower wall. The drag force relaxes the individual molecular velocity to the local macroscopic velocity in a characteristic

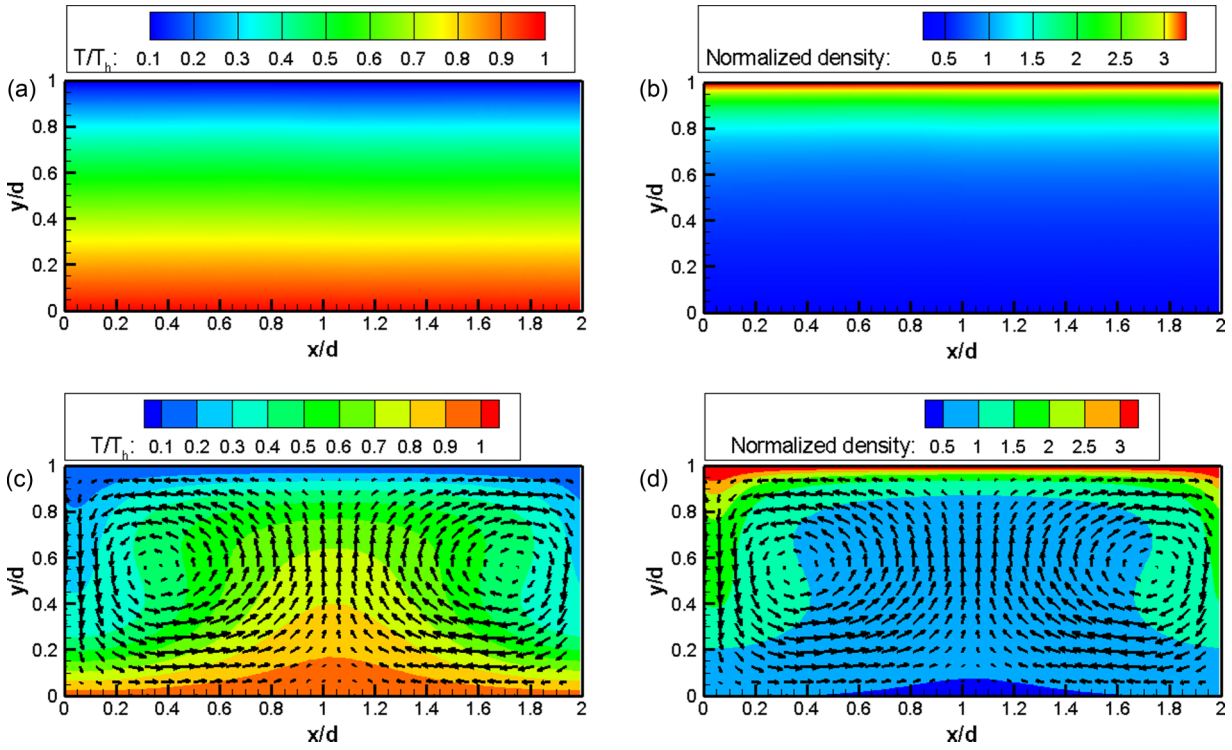

FIG. 2. Temperature and density fields for Ra = 1600 and Ra = 4000: (a) temperature field for Ra = 1600, (b) density field for Ra = 1600, (c) temperature field for Ra = 4000, and (d) density field for Ra = 4000. Velocity vectors are also shown when a convection pattern is formed at Ra = 4000.

time scale τ. It is obvious that the effect of gravity and the drag force is to generate collective velocity. The random force, on the other hand, adds thermal fluctuations to the molecular velocities and makes the molecular motions disordered. For a RB flow with a certain Ra, the competition between the collective effect and random effect determines the final pattern. When Ra is small, the random effect dominates over the collective effect, so the molecules are in a disordered state and there is no macroscopic motion. When Ra exceeds the critical value, the collective effect becomes dominant and thus the molecules tend to an ordered state. This results in a convective pattern.

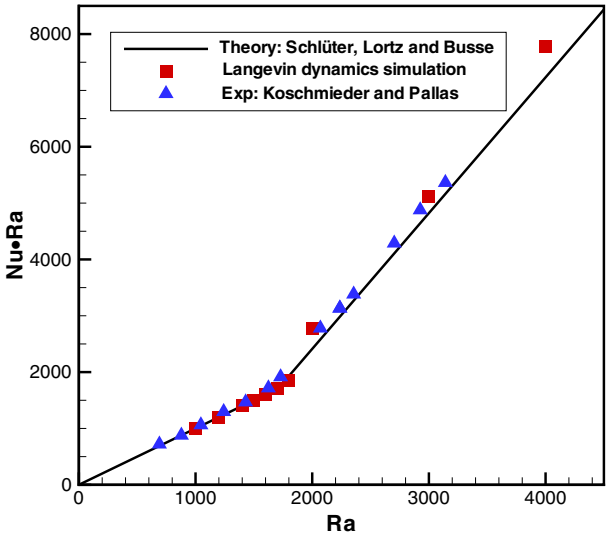

FIG. 3. Relation between Nu × Ra and Ra. The current results obtained by Langevin dynamics simulations are compared with theoretical and experimental results.

In order to reveal the separate effects of the drag force and the random force, we perform two sets of numerical tests. First, the role of the drag force is investigated by setting the local macroscopic velocity in Eq. (2) to zero instead of using the instantaneous value of the local macroscopic velocity calculated on the fly. In this way, there will be no convective motion, no matter how large Ra is. The reason for this is that the drag force term, making the individual molecular velocity relax to the local macroscopic velocity (it is enforced to be zero in this set of numerical tests), suppresses the generation of convective motions.

The second set of numerical tests is performed by dismissing the random term. Our simulations show that the convective motions cannot form as well in the absence of the random term. This demonstrates that thermal fluctuations play an important role in triggering the instability. Theoretically, the characteristics of thermal fluctuations in the RB system can be investigated using fluctuating hydrodynamics [14], in which the fluctuations are described by the usual hydrodynamic equations supplemented with random noise terms. Numerous theoretical analyses [14] based on fluctuating hydrodynamics have proved that the fluctuations are long-range correlated in the RB system, even far away from the onset of instability. In this paper we directly measure the spatial correlations of the local macroscopic fluctuations in the RB system. The characteristic of fluctuation correlations in combination with the Langevin equation are expected to shed light on the mechanism of the RB instability.

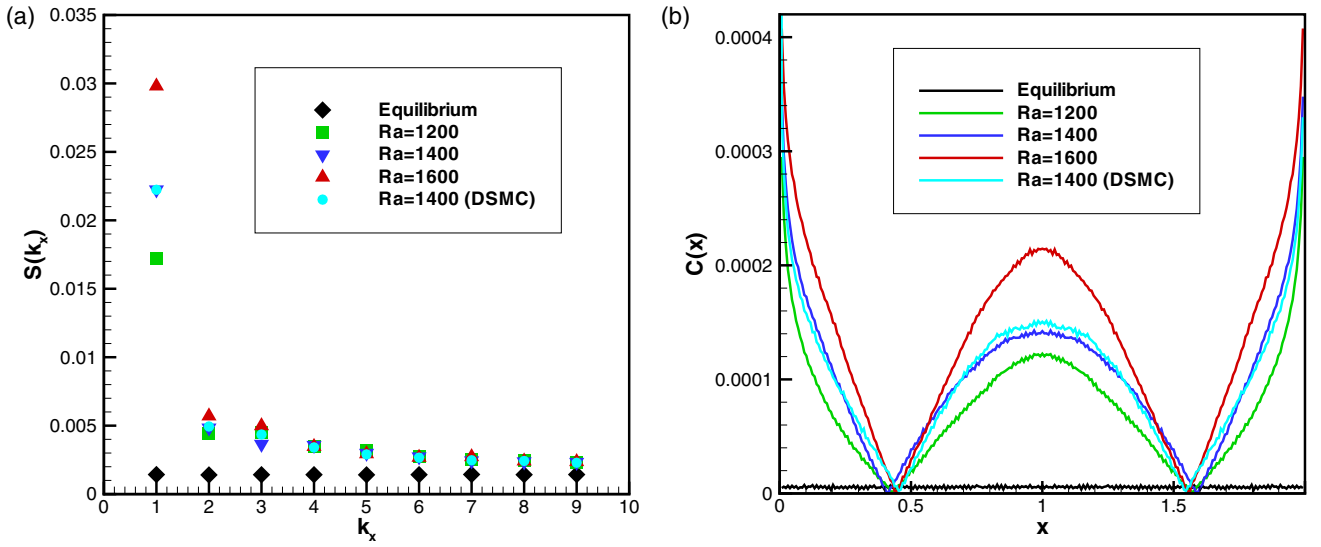

FIG. 4. Langevin simulation results of (a) the power spectrum and (b) the correlation function of the density fluctuations in the horizontal direction below the onset of the RB instability. For comparison, the DSMC result of Ra = 1400 under the same condition as the Langevin simulation is presented.

As a statistical method, the Langevin dynamics simulation method inevitably has statistical errors similar to the DSMC method. According to the theory of equilibrium statistical physics, the velocity for low-speed flows has a much lower signal-to-noise ratio than the density, so we measure the density fluctuations instead of the velocity fluctuations. In our simulations, the instant density field is obtained by taking an average over the number of molecules in discrete computational cells in one calculating time step. The density fluctuation (ρ') in each cell is then determined as the difference between the instant density (ρ) and the average density ($\rho_{\rm av}$), i.e., $\rho' = \rho - \rho_{\rm av}$. Considering that the boundary condition is periodic in the horizontal direction, it is straightforward to determine the power spectrum of fluctuations by applying the fast Fourier transform (FFT) to the fluctuating density data along the horizontal directions at each fixed y and each instant of time. To reduce the statistical noise, we average the power spectrums over y and 1000 different time instants. The spatial correlations in real space are then obtained by applying inverse FFT to the averaged power spectrum.

Figure 4(a) shows the power spectrum $S(k_x)$ of the normalized density fluctuations ($\rho'/\rho_{\rm av}$) for various Rayleigh numbers below the onset of instability, where k_x is the discrete wave number in the horizontal direction. It is shown that for any Ra the power spectrum at $k_x = 1$ is dominant, while in equilibrium there is no preferred discrete wave number. Furthermore, as Ra approaches the critical value, the intensity of the power spectrum at $k_x = 1$ continuously increases. This means that our simulations predict the critical discrete wave number as 1. For the sake of comparison with linear stability analysis, we change the discrete wave number k_x to the continuous wave number α_x using the relation $\alpha_x = \frac{2\pi k_x}{L}$, where L is the dimensionless length of the RB system. Using $k_x = 1$ and $L = 2$ (for our simulation setup) in the above equation, it predicts that the critical wave number α_x^c in continuous space is about 3.142, which is close to the prediction based on linear stability analysis ($\alpha_x^c = 3.117$). To validate our Langevin simulation results, we employ the DSMC method to simulate RB flows under the same conditions. As shown in Fig. 4(a), the results for Ra = 1400 obtained by DSMC and Langevin simulations are consistent. Our results are also in agreement with Wu *et al.*'s conclusion based on experiments [15], which demonstrated that the intensity of fluctuations below the onset of the convection has the maximum value at the critical wave number. It can also be seen that for higher wave numbers ($k_x > 4$), all the data for three different Ra tend to be the same. This characteristic is consistent with the theoretical prediction [28] based on fluctuating hydrodynamics, although direct comparison between our simulations and the theory is unachievable at present due to the non-Boussinesq effect in our simulations. Simulation works under the Boussinesq assumption could be done in the future to compare with theoretical prediction.

Figure 4(b) shows the spatial correlation function $C(x)$ of the density fluctuations, where x represents the distance between the two points along the horizontal direction. It is obvious that in equilibrium the fluctuations are short ranged. On the contrary, for the nonequilibrium state with a certain Ra, the fluctuations are long-range correlated. Specifically, the correlation first decreases with the distance and then increases until half of the length in the horizontal direction is reached, and it is symmetric with respect to the line at $x = 1$. Again, the Langevin simulation result for Ra = 1400 is consistent with the DSMC result under the same computational condition. Figure 4(b) also shows that the intensity of fluctuation correlations increase with Ra. The form of the fluctuation correlation is similar to that of a pair of counter-rotating vortices in a thermal convection state. In this context, we can conclude that the fluctuation correlations below the RB instability point already foreshadow to some extent the ultimate appearance of the convective pattern above the onset of instability.

Now we can elucidate the mechanism of the RB instability using the Langevin equation in conjunction with the

characteristic of fluctuation correlations. In the Langevin equation, the drag force term relaxes the individual molecular velocity u to the local instant macroscopic velocity U in a characteristic time scale τ. Even below the critical point, the local instant velocity is not zero but fluctuating all the time. More important, the fluctuating velocities are also long-range correlated in a form similar to the density fluctuations shown above. As Ra approaches the critical value, the fluctuation correlations continuously increase. When Ra is over the critical point, the individual molecular motions tend to their local collective motions with strong spatial correlations, and a convective pattern is finally formed.

IV. CONCLUSIONS

In this paper we employed the Langevin model to study the Rayleigh-Bénard instability problem, assuming that each molecule in the system is a Brownian particle colliding with its surrounding molecules. Our Langevin dynamics simulations reproduced the onset of thermal instability changing from a conductive to a convective state very well. The roles of the drag force and the random force terms in the Langevin equation in triggering thermal instability are elucidated via numerical tests. Furthermore, we demonstrated that the strength of the fluctuation correlations increases as the Rayleigh number approaches the critical value, and the characteristic of the fluctuation correlations determines the convective patterns formed above the critical Rayleigh number. Our latest studies showed that the Langevin equation can also be applied to simulate other flow instability problems, such as Kolmogorov flow [6] and Rayleigh-Taylor instability [29]. It is expected that researches in this direction will shed new light on the general mechanism of flow instability.

ACKNOWLEDGMENTS

This work was supported by the National Natural Science Foundation of China (Grants No. 11772034 and No. 11372325). J.Z. would like to thank Jing Fan and Fei Fei for stimulating discussions.

[1] S. Chandrasekhar, *Hydrodynamic and Hydromagnetic Stability* (Clarendon, Oxford, 1961).
[2] G. Ahlers, S. Grossmann, and D. Lohse, Rev. Mod. Phys. **81**, 503 (2009).
[3] D. Lohse and K.-Q. Xia, Annu. Rev. Fluid Mech. **42**, 335 (2010).
[4] G. Nicolis and I. Prigogine, *Self-Organization in Nonequilibrium Systems* (Wiley, New York, 1977).
[5] H. Haken, *Synergetics: An Introduction. Nonequilibrium Phase Transitions and Self-Organization in Physics, Chemistry and Biology* (Springer-Verlag, Berlin, 1983).
[6] A. Manela and J. Zhang, J. Fluid Mech. **694**, 29 (2012).
[7] M. A. Gallis, T. P. Koehler, J. R. Torczynski, and S. J. Plimpton, Phys. Fluids **27**, 084105 (2015).
[8] M. A. Gallis, N. P. Bitter, T. P. Koehler, J. R. Torczynski, S. J. Plimpton, and G. Papadakis, Phys. Rev. Lett. **118**, 064501 (2017).
[9] S. Stefanov, V. Roussinov, and C. Cercignani, Phys. Fluids **14**, 2255 (2002).
[10] J. Zhang and J. Fan, Phys. Rev. E **79**, 056302 (2009).
[11] A. Puhl, M. M. Mansour, and M. Mareschal, Phys. Rev. A **40**, 1999 (1989).
[12] D. C. Rapaport, Phys. Rev. E **73**, 025301(R) (2006).
[13] A. García and C. Penland, J. Stat. Phys. **64**, 1121 (1991).
[14] J. M. O. De Zarate and J. V. Sengers, *Hydrodynamic Fluctuations in Fluids and Fluid Mixtures* (Elsevier, Amsterdam, 2006).
[15] M. Wu, G. Ahlers, and D. S. Cannell, Phys. Rev. Lett. **75**, 1743 (1995).
[16] P. Jenny, M. Torrilhon, and S. Heinz, J. Comput. Phys. **229**, 1077 (2010).
[17] M. H. Gorji and P. Jenny, J. Comput. Phys. **262**, 325 (2014).
[18] M. H. Gorji, M. Torrilhon, and P. Jenny, J. Fluid Mech. **680**, 574 (2011).
[19] T. Önskog and J. Zhang, Physica A **440**, 139 (2015).
[20] F. Fei, Z. Liu, J. Zhang, and C. Zheng, Commun. Comput. Phys. **22**, 338 (2017).
[21] E. Golshtein and T. Elperin, J. Thermophys. Heat Transfer **10**, 250 (1996).
[22] A. Manela and I. Frankel, Phys. Fluids **17**, 036101 (2005).
[23] G. Bird, *Molecular Gas Dynamics and the Direct Simulation Monte Carlo of Gas Flows* (Clarendon, Oxford, 1994).
[24] J. Zhang, D. Zeng, and J. Fan, Physica A **411**, 104 (2014).
[25] J. Zhang and J. Fan, Chin. Sci. Bull. **54**, 364 (2009).
[26] A. Schlüter, D. Lortz, and F. Busse, J. Fluid Mech. **23**, 129 (1965).
[27] E. Koschmieder and S. Pallas, Int. J. Heat Mass Transfer **17**, 991 (1974).
[28] J. M. O. De Zarate and J. V. Sengers, Physica A **300**, 25 (2001).
[29] M. A. Gallis, T. P. Koehler, J. R. Torczynski, and S. J. Plimpton, Phys. Rev. Fluids **1**, 043403 (2016).